Measurement Analysis of NLOS Indoor MIMO Channels

Kai Yu[1] **Mats Bengtsson**[1] **Björn Ottersten**[1] **Peter Karlsson**[2]
Darren McNamara[3] **Mark Beach**[3]

[1] Department of Signals, Sensors and Systems
Royal Institute of Technology, Stockholm, Sweden
Email: kaiyu@s3.kth.se

[2] Telia Research AB, Malmö, Sweden

[3] Center for Communication Research,
University of Bristol, United Kingdom

Abstract: *In this paper, we present results from measurements conducted by the University of Bristol. We study the channel characteristics of Multiple-Input-Multiple-Output (MIMO) indoor channel at 5.2 GHz. Our investigation shows that the envelope of the channel for non-line-of-sight (NLOS) indoor situations is approximately Rayleigh distributed and consequently we focus on a statistical description of the first and second order moments of the narrowband MIMO channel. Furthermore, it is shown that for NLOS indoor scenarios, the MIMO channel covariance matrix can be well modeled by a Kronecker product of the covariance matrices describing the correlation at the transmitter and the receiver side respectively. A statistical narrowband model for the NLOS indoor MIMO channel based on this covariance structure is presented along with some simulation results.*

1. Introduction.

It is well known that using antenna arrays at both the transmitter and receiver over a MIMO channel can provide very high channel capacity as long as the environment can provide sufficiently rich scattering. Under these circumstances, the channel matrix elements have low correlation leading to channel realizations of high rank and consequently provide substantial channel capacity increases. In [1] and [2] the channel capacity for MIMO systems has been investigated theoretically and in [3] an architecture for MIMO system has been proposed. Some experimental results have been reported to characterize the MIMO channel and the corresponding capacity, see [4, 5, 6, 7, 8].

There is of course great interest in MIMO channel modeling. A so-called one-ring model has been proposed and investigated in [9]. In [10], a distributed scattering model has been proposed in order to explain the 'pinhole' phenomenon that sometimes happens in long distance outdoor situations. In [11], a model based on channel power correlation coefficients is presented. However, models based on measured data are still rare.

In this paper, we report the results from measurements conducted at 5.2 GHz by the University of Bristol. A statistical narrowband model for the NLOS indoor MIMO channel based on the channel covariance structure is presented. The rest of the paper is organized as follows: In section II, the measurement setup is described, including the test environment, the test equipment and some important parameters. Section III presents a second order statistical structure and an optimal matrix separation method. A statistical model based on above structure and the results from model identification are presented in section IV. Finally we draw the conclusions in section V.

2. Measurement System

The test site is the Merchant Venture's Building (MVB) of the University of Bristol. The general layout of the test site includes office rooms, computer labs, corridors and open spaces. There are 15 transmitter locations and 3 receiver locations during the entire measurements, including both line-of-sight (LOS) and NLOS cases. However, all the results reported in this paper are from NLOS cases as shown in Fig. 1, where the transmitter is located in a computer lab and the receiver is at the corner of a large modern office with cubicles.

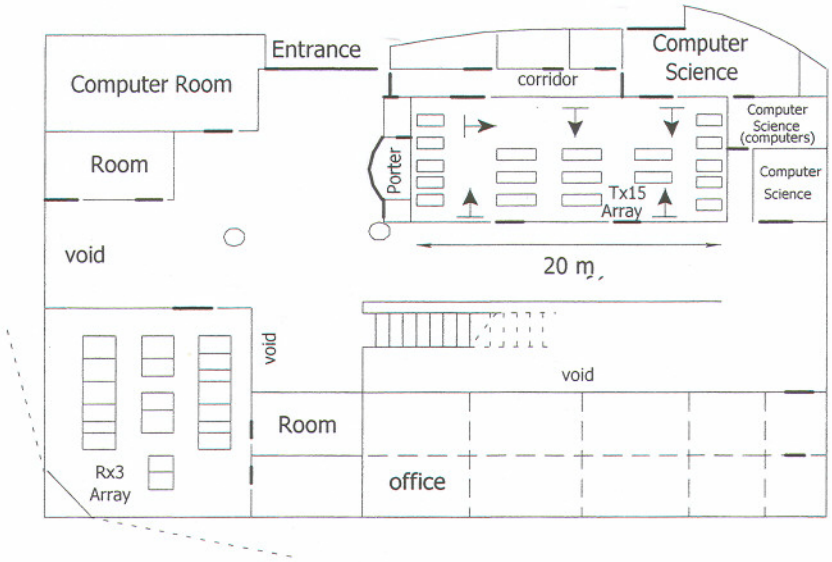

Figure 1. Measurement scenario for NLOS indoor MIMO channel

The measurements were carried out using the Medav RUSK BRI vector sounder, which has 8-element omnidirectional uniform linear array (ULA) at the transmitter side and 8-element ULA with 120° beamwidth at the receiver side. The distance between two neighboring antenna elements is 0.5λ at both ends. There is a feedback from the receiver to the transmitter by cables in order to synchronize the transmitter and receiver.

The measurements were centered at 5.2 GHz with a 120 MHz bandwidth. The excess delay window is $0.8\mu s$, which corresponds to 97 frequency subchannels. For each transmit element, one 'vector snapshot' (one measurement from each receive element) is taken at the receiver. The sampling time for one complete MIMO snapshot (8 vector snapshots) is $102.4\mu s$. One complete measurement includes 199 blocks with 16 MIMO snapshots within each block, therefore there are 3184 complete MIMO snapshots in total for each frequency subchannel. The time delay between two neighboring blocks is 26.624ms. This means the total time for one complete measurement is 5.2s. During the measurements, people were moving around both at the transmitter side and receiver side. The test signal was sent out by the transmitter and captured by the receiver, the impulse response of the channel was then saved in the frequency domain. More details about the measurements can be found in [8].

3. Measurement Analysis Method

Assume there are m transmit elements and n receive elements. For a narrowband MIMO channel, the input-output relationship could be expressed in the baseband as

$$\mathbf{y}(t) = \mathbf{H}_n^m \mathbf{s}(t) + \mathbf{n}(t)$$

where $\mathbf{s}(t)$ is the transmitted signal, $\mathbf{y}(t)$ is the received signal and $\mathbf{n}(t)$ is additive white Gaussian noise (AWGN). The channel matrix $\mathbf{H}_n^m$ here is an n by m matrix.

Channel Capacity and Normalization Method

When the transmitter has no information about the channel, a straightforward way is to allocate the power equally to each transmit element. The corresponding channel capacity is given by [2]

$$C = \log_2 \det(\mathbf{I}_n + \frac{\rho}{m}\mathbf{H}_n^m \mathbf{H}_n^{m^*}) \quad (1)$$

where $\mathbf{H}_n^m$ is the normalized channel matrix, ρ is the average signal-to-noise ratio at each receiver branch and '*' denotes complex conjugate transpose. To get the normalized channel matrix, we normalize the measured MIMO snapshots by a common factor such that

$$E[\left\|\mathbf{H}_n^m\right\|_F^2] = nm \quad (2)$$

where $\left\|\cdot\right\|_F$ denotes Frobenius norm and E[·] denotes the expected value.

Covariance Matrix Estimation

In [11], it is claimed that the correlation between the power of two subchannels could be modeled by the product of the correlations seen from the transmitter and receiver. Here we try to verify whether this structure could be extended to include also the phase of the complex valued amplitudes as assumed in [9, 13]. Notice that for normalized channel matrix $\mathbf{H}_n^m$, this means that

$$\mathbf{R}_H = \mathbf{R}_H^{Tx} \otimes \mathbf{R}_H^{Rx}, \quad (3)$$

where '$\otimes$' denotes Kronecker product and we define the transmitter, receiver and channel covariance matrices as follows

$$\mathbf{R}_H^{Tx} = E[(\mathbf{h}_i^* \mathbf{h}_i)^T] \quad \text{for } i = 1, \ldots, n \quad (4)$$

$$\mathbf{R}_H^{Rx} = E[\mathbf{h}^j \mathbf{h}^{j^*}] \quad \text{for } j = 1, \ldots, m \quad (5)$$

$$\mathbf{R}_H = E[\mathrm{vec}(\mathbf{H}_n^m)\mathrm{vec}(\mathbf{H}_n^m)^*] \quad (6)$$

where $\mathbf{h}_i$ is ith row of $\mathbf{H}_n^m$, $\mathbf{h}^j$ is jth column of $\mathbf{H}_n^m$, 'T' is transpose and vec(·) is the '*vec*' operator.

Matrix Separation Method

In order to show how well the above Kronecker product holds, we present an optimal method to separate the channel matrix $\mathbf{R}_H$ into the Kronecker product of two Hermitian matrices $\mathbf{X}$ and $\mathbf{Y}$. This separation problem could be written as

$$\min \left\|\mathbf{R}_H - \mathbf{X} \otimes \mathbf{Y}\right\|_F \quad (7)$$

The least squares rank one approximation method in [12] could be used to solve this problem. The main idea is to re-arrange the elements of the covariance matrix $\mathbf{R}_H$ and $\mathbf{X} \otimes \mathbf{Y}$ simultaneously to get a least squares problem of the form

$$\min \left\|\mathbf{R}_{tran} - \mathbf{x}(\mathbf{y}^c)^*\right\|_F \quad (8)$$

where $\mathbf{x} = \mathrm{vec}(\mathbf{X})$ and $\mathbf{y} = \mathrm{vec}(\mathbf{Y})$, '$c$' means complex conjugate and $\mathbf{R}_{tran}$ is the transformed matrix of $\mathbf{R}_H$.

To get this transformed matrix $\mathbf{R}_{tran}$, we use the permutation matrix $\mathbf{T}$, defined such that

$$\mathbf{T}\mathrm{vec}(\mathbf{X} \otimes \mathbf{Y}) = \mathrm{vec}(\mathbf{x}\mathbf{y}^T)$$

for all matrices $\mathbf{X}$ and $\mathbf{Y}$. The matrix $\mathbf{R}_{tran}$ is then defined as

$$\mathrm{vec}(\mathbf{R}_{tran}) = \mathbf{T}\mathrm{vec}(\mathbf{R}_H)$$

Note that problem (7) and (8) are equivalent since $\mathbf{T}$ is orthonormal. The solution to the least squares rank one approximation of $\mathbf{R}_H$ in (8) is easily calculated using the singular value decomposition (SVD). Let λ_{max} be the largest singular value of $\mathbf{R}_{tran}$, with the corresponding left and right singular vectors $\mathbf{u}_{max}$ and $\mathbf{v}_{max}$ respectively, then $\mathbf{x}$ and $\mathbf{y}$ could be expressed as

$$\mathbf{x} = \gamma \mathbf{u}_{max}$$

$$\mathbf{y}^c = \gamma^{-1} \lambda_{max} \mathbf{v}_{max}$$

where γ is an arbitrary scalar. Then it is straightforward to transform the two vectors $\mathbf{x}$ and $\mathbf{y}^c$ back to $\mathbf{X}$ and $\mathbf{Y}$.

It can be shown that the solution $\mathbf{X}$ and $\mathbf{Y}$ will always be Hermitian as long as $\mathbf{R}_H$ is Hermitian. Thus, it is not necessary to force that structure on the solution.

4. Measurement Results

As stated in section II, the measurements use an 8-element transmitter and receiver. However, only pairs of 2 neighboring elements at both the transmitter and receiver have been used to get 2 by 2 channel matrices in this paper. Similar results have been found for other setups with more elements. It is interesting to find that even though people were moving around during the measurements, the situation is still quite stationary. Therefore the results have been averaged both in the frequency and spatial domain, i.e. all the snapshots from different frequency subchannels (each subchannel is around 1.2 MHz) and spatial arrangements (at the same Tx and Rx position) have been seen as different channel realizations in order to get sufficient realizations to analyze the distribution and second order statistics of channel coefficients. All the realizations have been normalized by the same factor so that equation (2) holds on the average. In the following section, we use Tx15 -- Rx3 as an example, see Fig. 1. Similar results have been found for the other four transmitter locations as shown in the figure.

Envelope Distribution of Channel Coefficients

The channel characteristics has been investigated by plotting the histogram of the envelope of each channel coefficient. Fig. 2 shows the result of one channel coefficient between Tx15 – Rx3 along with a fitted Rayleigh envelope. It is shown that Rayleigh envelope fits the histogram very well and therefore we conclude that the channel envelope is Rayleigh distributed.

Second Order Statistics

It is well known that for a complex Gaussian distributed channel, the statistical information is completely described by its first and second order moments. Since the channel is complex Gaussian, we therefore focus on the second order statistics for this NLOS indoor scenario. First, we define the model error, Ψ to evaluate the difference between two matrices $\mathbf{A}$ and $\mathbf{B}$

$$\psi(\mathbf{A},\mathbf{B}) = \frac{\|\mathbf{A}-\mathbf{B}\|_F}{\|\mathbf{A}\|_F}$$

From the measured data, we investigate two model errors, the results are

$$\psi(\hat{\mathbf{R}}_H, \mathbf{X} \otimes \mathbf{Y}) = 4.83\%$$

$$\psi(\hat{\mathbf{R}}_H, \hat{\mathbf{R}}_H^{Tx} \otimes \hat{\mathbf{R}}_H^{Rx}) = 4.94\%$$

where the '^' indicates a sample covariance estimate of the corresponding quantities in equation (4), (5) and (6).

It is also interesting to see the difference between the optimal separation and those calculated from measured data. The scalar γ in the optimal separation is determined by using the least

squares method that fits all elements between two matrices optimally. The results are shown as follows

$$\psi(\hat{\mathbf{R}}_{\mathbf{H}}^{\mathbf{Tx}}, \mathbf{X}) = 1.36\%$$

$$\psi(\hat{\mathbf{R}}_{\mathbf{H}}^{\mathbf{Rx}}, \mathbf{Y}) = 0.30\%$$

From the above investigations, it is clearly shown that the channel covariance matrix could be well approximated by equation (3) and this structure could explain above 95% of the received signal power in this case.

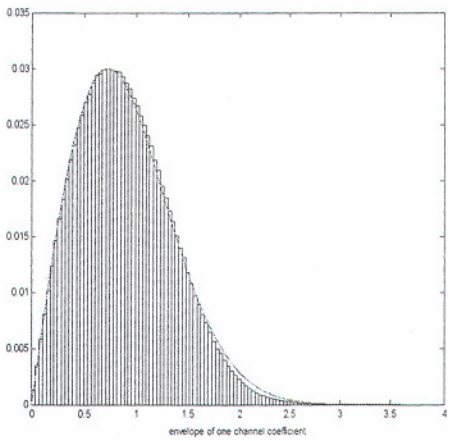

Figure 2. Histogram of envelope of one channel coefficient for NLOS indoor MIMO scenario and the fitted Raleigh distribution envelope (normalized)

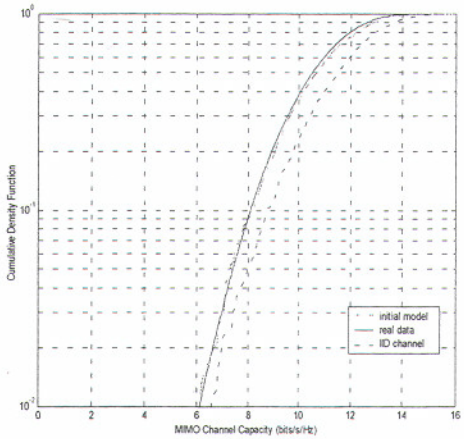

Figure 3. Cumulative density function of channel capacity for measured data, statistical model and IID MIMO channel. The SNR at the receiver side is 20dB. Power is equally allocated to transmit elements.

Statistical Model and Simulations

Since the channel coefficients are complex Gaussian, it is easy to show from equation (3) that the channel could be modeled as

$$\mathbf{H} = (\mathbf{R}_{\mathbf{H}}^{\mathbf{Rx}})^{1/2}\mathbf{G}((\mathbf{R}_{\mathbf{H}}^{\mathbf{Tx}})^{1/2})^{\mathbf{T}}$$

where **G** is a stochastic M by N matrix with independent and identically distributed (IID) $CN(0,1)$ elements. Here $(\cdot)^{1/2}$ is any matrix square root such that $\mathbf{R}^{1/2}(\mathbf{R}^{1/2})^{*} = \mathbf{R}$. Notice that this model has already been assumed in [13] to study the channel capacity and it is also a special case of the model given in [10].

Monte-Carlo computer simulations have been used to generate 1000 channel realizations and the cumulative density function (CDF) of the channel capacity between those from measured data and from simulated channel realizations are compared. The results are given in Fig. 3. The capacity for the IID channel is also included as a reference. It is shown that the CDF from simulated channel realizations fits the CDF from the measured data quite well, which agrees with this model.

5. Conclusions

We access the data measured by the University of Bristol. Our investigation shows that for NLOS indoor MIMO scenarios, the envelope of the narrowband channel coefficients are approximately Rayleigh distributed. Furthermore, it shows that the channel covariance matrix could be well approximated by the Kronecker product of the covariance matrices at the transmitter side and the receiver side. We also introduce a narrowband model for the NLOS

indoor MIMO channel based on this second order statistical structure. Monte-Carlo simulations show the agreement between measured data and this model.

Acknowledgement

This work is conducted in part within the project SATURN (Smart Antenna Technology in Universal bRoadband wireless Networks) funded by the EU IST program.

References

[1] I. Emre Telatar, "Capacity of multi-antenna Gaussian channels," *European Transactions on Telecommunications*, vol.10, no. 6, pp. 585-595, Nov/Dec. 1999.

[2] G. J. Foschini and M. J. Gans, "On limits of wireless communications in a fading environment," *Wireless Personal communications*, vol.6, pp. 311-335, 1998.

[3] G. J. Foshini, "Layered space-time architecture for wireless communication in a fading environment when using multiple antenna," *Bell Laboratories Technical Journal*, vol.1, no. 2, pp. 41-59, 1996.

[4] Jean Philippe Kermoal, Laurent Schumacher, Preben E. Mogensen, and Klaus I. Pedersen, "Experimental investigation of correlation properties of MIMO radio channels for indoor picocell scenarios," in *Proceedings IEEE Vehicular Technology Conference*, IEEE VTC Fall, 2000.

[5] Carol C. Martin, Jack H. Winters, and Nelson R. Sollenberger, "Multiple-Input-Multiple-Output (MIMO) radio channel measurements," in *Proceedings IEEE Vehicular Technology Conference*, IEEE VTC Fall, 2000.

[6] Rickard Stridh, Peter Karlsson, and Björn Ottersten, "MIMO channel capacity on a measured indoor radio channel at 5.8 GHz," in *Proceedings of the Asilomar Conference on Signals, Systems and Computers*, October 2000.

[7] Rickard Stridh and Björn Ottersten, "Spatial characterization of indoor radio channel measurements at 5 GHz," in *Proceedings IEEE Sensor Array and Multichannel Signal Processing Workshop*, March 2000.

[8] D. P. McNamara, M. A. Beach, and P. N. Fletcher and P. Karlsson, "Initial Investigation of Multiple-Input Multiple-Output (MIMO) Channels in Indoor Environments," in *Proceedings IEEE Benelux Chapter Symposium on Communications and Vehicular Technology*, Leuven, Belgium, October 2000.

[9] Da-Shan Shiu, G. J. Foshini, M. J. Gans, and J. M. Kahn, "Fading correlation and its effect on the capacity of multielement antenna systems," *IEEE Transactions on Communications*, vol. 48, no. 3, pp. 502-513, March 2000.

[10] D. Gesbert, H. Bölcskei, D. Gore, and A. Paulraj, "MIMO wireless channels: capacity and performance," in *Proceedings Global Telecommunications* Conference, November 2000.

[11] K. I. Pedersen, J. B. Andersen, J. P. Kermoal, and P. Mogensen, "A stochastic Multiple-Input-Multiple-Output radio channel model for evaluation of space-time coding algorithms ," in *Proceedings IEEE Vehicular Technology Conference*, IEEE VTC Fall, 2000.

[12] Peter Strobach, "Low-rank detection of multichannel Gaussian signals using block matrix approximation," *IEEE Transactions on Signal Processing*, vol. 43, no. 1,pp. 233-242, January 1995.

[13] Dimitry Chizhik, Farrokh Rashid-Farrokhi, Jonathan Ling and Angel Lozano, "Effect of antenna separation on the capacity of BLAST in correlated channels," *IEEE Communications Letters*, vol.4, no. 11 November 2000.